Hidaka
Journal of Analytical Science and Technology (2024) 15:14
https://doi.org/10.1186/s40543-024-00424-6

Journal of Analytical Science and Technology

RESEARCH ARTICLE

Open Access

Isotopic variations of Sm, Gd, Er and Yb found in planetary materials caused by neutron-capture reactions in nature

Hiroshi Hidaka[1*]

Abstract

The isotopic shifts of ^{149}Sm–^{150}Sm and ^{157}Gd–^{158}Gd have often been observed in meteorites and lunar surface materials, because they result from the neutron-capture reactions associated with secondary neutrons produced by cosmic-ray irradiation. While the Sm and Gd isotopic shifts can mainly be used for the estimation of thermal neutron fluences that of ^{167}Er–^{168}Er has recently been applied in the estimation of epithermal neutron fluences. The systematic isotopic dataset of Sm, Gd and Er helps us to consider the details of planetary materials' cosmic-ray exposure conditions using the balance of the fluences between thermal and epithermal neutrons. This paper reviews a series of isotopic variations of Sm, Gd, and Er in association with neutron-capture reactions for the application of planetary sciences. As a new attempt and possibility for better understanding the neutron fluence and its energy distribution, the use of Yb isotopic variation is then discussed using two different data sources, namely lunar regolith and the Oklo natural reactors. Finally, the preliminary result for the precise isotopic measurement of Yb is presented from the viewpoint of chemical separation and instrumental improvement.

Keywords Neutron-capture, Cosmic-ray irradiation, Isotopic variations, Rare earth elements

Introduction

The surfaces of airless bodies of solar planets are exposed to cosmic rays. Spallation reactions by the interactions of cosmic rays with planetary materials produce spallogenic products, such as ^{10}Be and ^{53}Mn. Such spallogenic products, called cosmogenic nuclides, have been effectively used for understanding the cosmic-ray exposure (CRE) conditions of planetary materials (e.g., Nishiizumi et al. 1996). At the occurrence of spallation reactions, neutrons are produced. Neutrons produced by spallation gradually reduce their energy down to epithermal (0.1 eV $< E <$ 0.5 MeV) to thermal ($E <$ 0.1 eV) energy regions by a collision cascade with the surrounding atoms in the planetary materials. Energy-lost neutrons then become more reactive with the nuclei consisting of the planetary materials. Neutron capture is one of the major reactions caused by cosmic-ray irradiation to the surficial parts of planetary bodies in space.

The total amount of neutrons produced in a target material by the cosmic-ray interaction and its energy distribution are highly dependent on the chemical composition and the size of the target material in space; therefore, their quantitative evaluations are important for better understanding the surficial changes of materials during the evolution processes of planets.

Several isotopes of some rare earth elements (REEs) have significantly large neutron-capture cross sections. In addition, isotopic abundances have changed as the neutron-capture reactions accumulate. For example, ^{149}Sm and ^{157}Gd react sensitively with thermal neutrons ($E <$ 0.1 eV), and become ^{150}Sm and ^{158}Gd, respectively. The degrees of the ^{149}Sm–^{150}Sm and ^{157}Gd–^{158}Gd

*Correspondence:
Hiroshi Hidaka
hidaka@eps.nagoya-u.ac.jp
[1] Department of Earth and Planetary Sciences, Nagoya University, Nagoya 464-8601, Japan

isotopic shifts can be used as a neutron dosimeter of the thermal neutrons produced in association with cosmic-ray irradiation. On the other hand, because ^{167}Er reacts with epithermal neutrons (0.1 eV < E < 500 keV) as well as thermal neutrons, the isotopic shift of ^{167}Er–^{168}Er can be used for dosimetry of the epithermal neutrons. Systematic isotopic analyses of Sm, Gd, and Er collected from the same single material are planned to obtain information on neutron fluences in an energy range from the thermal to epithermal regions, which will provide information about the surface conditions of the cosmic-ray irradiated planetary materials.

This paper reviews a series of isotopic studies of Sm, Gd and Er for the application of planetary sciences and then, discusses new attempts to evaluate the occurrence of neutron-capture reactions in nature using Yb isotopic variations. Considering the nuclear properties of ^{168}Yb, the isotopic depletion degree of ^{168}Yb associated with the neutron-capture reaction of ^{168}Yb(n,γβ$^+$)^{169}Tm could also be used in the application of an epithermal neutron dosimeter. The determination of Yb isotopic composition for planetary materials has been examined for a better understanding of nucleosynthetic heritage in the solar system (Shollenberger et al. 2018; Shollenberger and Brennecka 2020), mass-dependent fractionation in association with the condensation of the formation of planetary materials (Albalat et al. 2012, 2015), and estimation for the β$^+$ decay of ^{176}Lu to ^{176}Yb (Amelin and Davis 2005). In this paper, however, the development of precise isotopic analysis of Yb is managed for the detection of the isotopic depletion of ^{168}Yb derived from the neutron-capture reaction of ^{168}Yb(n,γβ$^+$)^{169}Tm. In association with the neutron-capture reactions, the Yb isotopic approach is somewhat more complicated for quantitative discussions than those of Sm, Gd, and Er, because the neutron-capture reaction of ^{168}Yb is not (n,γ)-type but (n,γβ$^+$)-type reaction. ^{168}Yb converts to a different element ^{169}Tm by the neutron-capture reaction. In addition, ^{169}Tm has a larger epithermal neutron-capture cross section, σ_{epi}, than thermal neutron-capture cross section, σ_{th}, and converts to ^{170}Yb by the neutron-capture reaction of ^{169}Tm(n,γβ$^-$)^{170}Yb. As a reference, the Yb isotopic compositions of the Oklo natural fission reactor materials, which are known to be intensively irradiated with neutrons, show a small but significant deficit of ^{168}Yb by ^{168}Yb(n,γβ$^+$)^{169}Tm and enrichment of ^{170}Yb produced from ^{169}Tm(n,γβ$^-$)^{170}Yb (Holliger and Devillers 1981; Hidaka and Holliger 1998). It is interesting to find the isotopic variations of ^{168}Yb and ^{170}Yb in extraterrestrial materials and consider their application for neutron dosimetry in nature. Because the isotopic abundances of both ^{168}Yb and ^{170}Yb are originally small (0.13% and 3.04% of the total, respectively), careful and precise measurements should be required to detect their isotopic variations. Hidaka et al. (2020) examined the determination of Yb isotopic compositions of a series of lunar regolith samples collected from a 2.4 m-length drill stem at the Apollo 15 (A-15) landing site and reported the resolvable ^{168}Yb isotopic depletions in four of seven samples.

Background for neutron-capture reactions

Neutron energy spectra

Considering the large thermal neutron-capture cross section of ^{149}Sm and ^{157}Gd, the isotopic variation of ^{150}Sm/^{149}Sm and/or ^{158}Gd/^{157}Gd have been used to evaluate the thermal neutron fluences in the target materials (Lingenfelter et al. 1972; Russ et al. 1972). Considering the variations in neutron fluence alongside energy, the neutron energy spectrum arising in the planetary materials by cosmic-ray irradiation is known to have dependencies on the chemical composition and the size of the target materials irradiated by cosmic rays (e.g., Spergel et al. 1986). In a previous study on the estimation of neutron fluences of planetary materials, thermal neutrons are considered to be more dominant than epithermal neutrons. However, there are few quantitative discussions about epithermal neutron fluences. Nevertheless, evaluation of the epithermal neutron fluence is also important, because the shape of neutron energy spectra largely changes, especially in the epithermal energy region (0.1 eV < E < 0.5 MeV).

Neutron energy-dependency of neutron-capture cross section of nuclides

The neutron-capture cross section of each nuclide is often characterized as a function of the neutron energy. On the other hand, it generally decreases along with the $E^{-1/2}$ in the thermal energy region. Then, it has many sharp peaks, called resonance, in the epithermal energy region. For the evaluation of the reactivities of individual nuclides with neutrons in the resonance region, the resonance integral (RI) is defined as the following equation;

$$\mathrm{RI} = \int_{E_c}^{E_{max}} \sigma(E) \frac{\mathrm{d}E}{E} \tag{1}$$

where E_c is a cut-off energy, typically used as 0.5 eV, and E_{max} is the highest energy in the region of neutron-capture resonance, and $\sigma(E)$ is a neutron-capture cross section as a function of energy. From Eq. (1), the epithermal neutron-capture cross section, σ_{epi}, can be obtained as follows:

$$\sigma_{epi} = \frac{\mathrm{RI}}{\int_{E_c}^{E_{max}} \frac{\mathrm{d}E}{E}} \tag{2}$$

Detailed data for the neutron energy spectrum, thermal neutron-capture cross section, and RI for each

nuclide were mainly obtained from the Evaluated Nuclear Data File (ENDF) by USA and the Japanese Evaluated Nuclear Data Library (JENDL) compiled in national evaluated data libraries. Considering the balance of cross section between σ_{th} and σ_{epi}, ^{149}Sm, ^{157}Gd, ^{167}Er, ^{168}Yb and ^{169}Tm were selected as reasonable candidate nuclides for the evaluation of thermal and/or epithermal neutron fluences arising in planetary materials, in this study. The σ_{th} and σ_{epi} values for ^{149}Sm, ^{157}Gd, ^{167}Er, ^{168}Yb, and ^{169}Tm are listed in Table 1. Because the resonance peaks of the nuclides selected in Table 1 have different widths in the limited energy regions, the isotopic results are not enough to reproduce the neutron energy spectrum fully recovered in epithermal energy region. However, the purpose of this study is to provide hints for reconstructing a continuous neutron energy spectrum by combining the intermittent data from the several nuclides.

Table 1 The data for neutron-capture reactions of the selected nuclides in this study

	σ_{th} (barn)	RI (barn)	E_{max} (eV)	σ_{epi} (barn)[a]
^{149}Sm	4.01×10^{4}	3.38×10^{3}	600	4.77×10^{2}
^{157}Gd	2.53×10^{5}	7.59×10^{2}	2000	1.19×10^{2}
^{167}Er	6.49×10^{2}	2.98×10^{3}	2000	3.59×10^{2}
^{168}Yb	2.30×10^{3}	2.13×10^{4}	200	3.56×10^{3}
^{169}Tm	1.05×10^{2}	1.62×10^{3}	2000	1.95×10^{2}

Individual data are selected from Evaluated Nuclear Data File (ENDF/B-VIII.0) and Japanese Evaluated Nuclear Data Library (JENDL-5) compiled by Brookhaven National Laboratory

[a] The epithermal cross section (σ_{epi}) is calculated from the Eq. (2) (see text) with the parameters RI and ε_{max} in the table

Isotopic variations of Sm, Gd, and Er caused by neutron-capture reactions

Sm isotopic shift of ^{149}Sm–^{150}Sm

Samarium has seven stable isotopes with mass numbers, 144, 147, 148, 149, 150, 152, and 154. Considering a very large σ_{th} (4.2×10^{4} barn at $E=0.0253$ eV) relative to a smaller σ_{epi} (4.77×10^{2} barn at 0.5 eV$<E<$600 eV) for ^{149}Sm, an isotopic shift from ^{149}Sm to ^{150}Sm by the neutron-capture reaction of ^{149}Sm(n,γ)^{150}Sm is predominantly affected by thermal neutrons. As the isotopic decrement of ^{149}Sm corresponds quantitatively to the isotopic increment of ^{150}Sm, the isotopic shift of Sm is conveniently shown as three-isotope diagram for ^{149}Sm/^{152}Sm vs. ^{150}Sm/^{152}Sm. Figure 1a shows a three-isotope diagram of Sm isotopic shifts found in a series of the A-15 lunar regolith core samples. In addition, as the quantitative correspondence between the isotopic decrements of ^{149}Sm and the increments of ^{150}Sm is balanced, the data points in the figure are plotted in a straight line with a slope of −1.

Based on the variation degree of the Sm isotopic shift, the total number of thermal neutrons, thermal neutron fluence Ψ_{th} (neutron number per square centimeter: n cm^{-2}), arising in planetary materials can be evaluated from the Sm isotopic shift as the following equation;

$$\Psi_{th} = \frac{1}{\sigma_{th}} \cdot \ln\left(\frac{1+R}{1+R_0}\right) \tag{3}$$

where $R_0 = ^{150}$Sm/^{149}Sm isotopic ratio without neutron-capture reactions (standard reference material), and $R = ^{150}$Sm/^{149}Sm isotopic ratio affected by neutron-capture reactions (Hidaka et al. 2020).

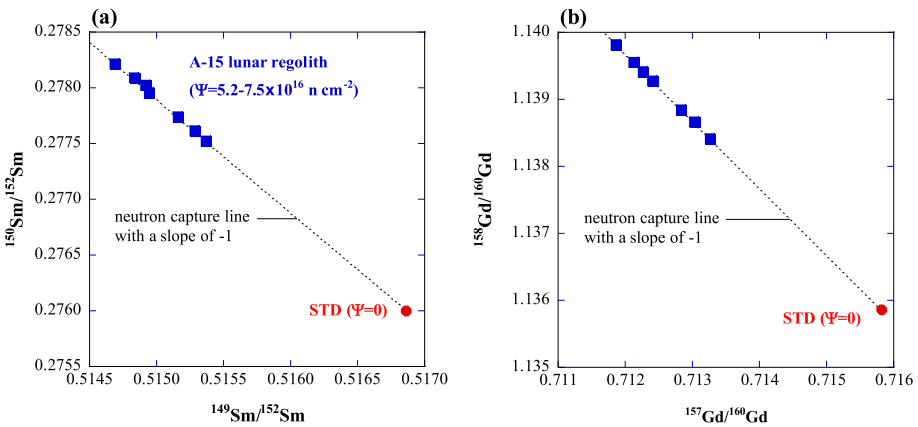

Fig. 1 Correlation diagrams **a** between ^{149}Sm/^{152}Sm and ^{150}Sm/^{152}Sm (Sm three-isotope plot) and **b** between ^{157}Gd/^{160}Gd and ^{158}Gd/^{160}Gd (Gd three-isotope plot) for a series of lunar regolith samples collected from the A-15 drill stem. The isotopic data are given by Hidaka et al. (2000)

Gd isotopic shift of ^{157}Gd–^{158}Gd

Gadolinium has seven stable isotopes with mass numbers 152, 154, 155, 156, 157, 158, and 160. Since ^{157}Gd has a very large σ_{th} (2.5×10^5 barn at $E=0.0253$ eV) and a small σ_{epi} (1.2×10^2 barn at 0.5 eV $< E <$ 300 eV), the isotopic shift of ^{157}Gd to ^{158}Gd can be treated similarly for the evaluation of Ψ_{th} as in the case of ^{149}Sm–^{150}Sm. Figure 1b shows a three-isotope diagram of Gd for the A-15 lunar samples. When comparing the neutron-capture cross section between ^{149}Sm and ^{158}Gd in detail, however, ^{149}Sm has a large resonance peak at 0.0973 eV with a slightly higher value in the thermal energy region, which suggests that ^{149}Sm not only react with well-thermalized neutrons but also slightly energetic neutrons. However, the cross section of ^{157}Gd does not show such resonance peaks in the thermal energy region. Using this difference found in the cross section between ^{149}Sm and ^{155}Gd, an index, $\varepsilon_{Sm}/\varepsilon_{Gd}$, consisting of the combination of Sm and Gd isotopic shifts was applied to discuss the energy distribution of neutrons within the thermal region (Lingenfelter et al. 1972; Russ et al. 1972). The index $\varepsilon_{Sm}/\varepsilon_{Gd}$ determining the thermalization degree of neutrons is given by the combination of Sm and Gd isotopic shifts as follows:

$$\frac{\varepsilon_{Sm}}{\varepsilon_{Gd}} = \frac{\left\{\left(\frac{^{150}Sm}{^{149}Sm}\right)_{meas} - \left(\frac{^{150}Sm}{^{149}Sm}\right)_{STD}\right\} \Big/ \left\{1 + \left(\frac{^{150}Sm}{^{149}Sm}\right)_{meas}\right\}}{\left\{\left(\frac{^{158}Gd}{^{157}Gd}\right)_{meas} - \left(\frac{^{158}Gd}{^{157}Gd}\right)_{STD}\right\} \Big/ \left\{1 + \left(\frac{^{158}Gd}{^{157}Gd}\right)_{meas}\right\}} \quad (4)$$

The cross sections of ^{149}Sm and ^{157}Gd vary with the chemical compositions of individual samples (Lingenfelter et al. 1972); therefore, the index $\varepsilon_{Sm}/\varepsilon_{Gd}$ is treated as a function of the effective total macroscopic cross section (Σ_{eff}) in consideration of the chemical composition of major elements, such as O, Si, Al, Fe, Ca, Mg, and Ti, and some effective trace elements, such as Cd, Eu, Sm, and Gd, in the matrixes of individual samples (Lingenfelter et al. 1972; Russ et al. 1972).

Er isotopic shift of ^{167}Er–^{168}Er

Erbium has six stable isotopes with mass numbers, 162, 164, 166, 167, 168, and 170. Since the neutron capture of ^{167}Er is also (n,γ)-type reaction, the history of neutron irradiation in each sample can be conveniently viewed by the three-isotope diagram between ^{167}Er/^{166}Er and ^{168}Er/^{166}Er. Comparing the size between σ_{th} (6.49×10^2 barn) and σ_{epi} (3.6×10^2 barn at 0.5 eV $< E <$ 2000 eV) of ^{167}Er, ^{167}Er can react with not only thermal neutrons but also epithermal neutrons. In this study, a total neutron fluence (Ψ) and total neutron-capture cross section (σ) are simply treated as the sum of thermal and epithermal components for fluence ($\Psi=\Psi_{th}+\Psi_{epi}$) and cross section ($\sigma=\sigma_{th}+\sigma_{epi}$), respectively. Modifying Eq. (3), the relationship between the Er isotopic shift R, Ψ, and σ is expressed as follows:

$$\Psi = \Psi_{th} + \Psi_{epi} = \frac{1}{\sigma}\cdot\ln\left(\frac{1+R}{1+R_0}\right) = \frac{1}{\sigma_{th}+\sigma_{epi}}\cdot\ln\left(\frac{1+R}{1+R_0}\right) \quad (5)$$

where $R_0=^{168}$Er/^{167}Er isotopic ratio without neutron-capture reactions (standard reference material), and $R=^{168}$Er/^{167}Er isotopic ratio affected by neutron-capture reactions (Hidaka et al. 2020). Here, $\sigma\Psi$ can be simply treated as $\sigma\Psi=\sigma_{th}\Psi_{th}+\sigma_{epi}\Psi_{epi}$, because $\sigma_{th}\Psi_{epi}$ and $\sigma_{epi}\Psi_{th}$ are negligible. Because Ψ_{th} can be evaluated from Sm and/or Gd isotopic shifts as expressed in Eq. (3), Ψ_{epi} can be quantified by the subtraction of Ψ_{th} from Ψ. Although the neutron-capture cross section of ^{167}Er is two orders of magnitude smaller than that of ^{149}Sm, the isotopic variations of ^{167}Er in the samples with $\Psi > 10^{16}$ *n* cm^{-2} are expected to be detectable and distinguishable between Ψ_{th} and Ψ_{epi} after subtraction of the contribution of Ψ_{th} evaluated from the Sm isotopic variations (Hidaka et al. 2020).

The systematic isotopic study of Sm, Gd, and Er provides information on the evaluation of Ψ_{th} and Ψ_{epi}, and the energy balance of neutrons within the thermal region based on the index $\varepsilon_{Sm}/\varepsilon_{Gd}$. Considering the size of the neutron-capture cross section as listed in Table 1, the isotopic variations of ^{168}Yb and ^{170}Yb are also expected to apply for the use of Ψ_{epi} dosimetry. Precise measurements of Yb isotopic composition are now being planned to establish the sensitive dosimeter for Ψ_{epi}. Here, in this study, new attempts to evaluate the occurrence of neutron-capture reactions observed in Yb isotopic variations will discuss.

Experimental procedures

Simulation of the isotopic variations of ^{168}Yb and ^{170}Yb

Ytterbium has seven isotopes with mass numbers 168, 170, 171, 172, 173, 174, and 176. Because the size of σ_{epi} (3.56×10^3 barn at 0.5 eV $< E <$ 200 eV) for ^{168}Yb is around one and a half times larger than that of σ_{th} (2.30×10^3 barn), ^{168}Yb reacts more sensitively with epithermal rather than thermal neutrons. Because ^{168}Yb becomes ^{169}Tm by the neutron-capture reaction of

^{168}Yb(n,γβ^{+})^{169}Tm, its reactivity can be evaluated from the isotopic depletion of ^{168}Yb.

On the other hand, Tm is a monoisotopic element having only one stable isotope ^{169}Tm. Because the size of σ_{epi} (1.95×10^{2} barn at 0.5 eV < E < 2000 eV) for ^{169}Tm is around two times larger than that of σ_{th} (1.05×10^{2} barn), ^{169}Tm reacts more sensitively with epithermal neutrons rather than thermal neutrons. As ^{169}Tm becomes ^{170}Yb through the neutron-capture reaction of ^{169}Tm(n,γβ^{-})^{170}Yb, its reactivity cannot be evaluated from the isotopic depletion of ^{169}Tm, but from the isotopic enrichment of ^{170}Yb. Evaluation of the epithermal neutron fluence arising in planetary materials can be expected from the possible detection of the quantitative degree of ^{170}Yb isotopic excess.

The disadvantageous point for the application of the presented two neutron-capture reactions is that their reactivities cannot be graphically viewed by a three-isotope diagram, because the two neutron-capture reactions are not (n,γ)-type. Considering the predominant reactivities of ^{168}Yb and ^{169}Tm with epithermal neutrons; however, precise measurements of Yb isotopic composition of cosmic-ray irradiated planetary materials are desired for the evaluation of Ψ_{epi} from the detection of both isotopic depletion of ^{168}Yb and excess of ^{170}Yb.

Hidaka et al. (2020) measured Yb isotopic compositions of the lunar regolith samples collected from the drill core at the A-15 landing site. A series of the core samples are known to be irradiated by a neutron fluence of $(5.2–7.5)\times10^{16}$ n cm^{-2} from the Sm isotopic shifts (Hidaka et al. 2000). As a result of Yb isotopic analyses of A-15 samples, four of seven samples in the A-15 core samples show isotopic depletions of ^{168}Yb, while the other three show less isotopic depletions than the analytical uncertainties. On the other hand, isotopic excesses of ^{170}Yb could not be identified in all seven samples from the A-15 core. One of the major reasons for unsatisfactory results in detecting the isotopic anomalies on ^{168}Yb and ^{170}Yb is insufficient analytical precisions of the isotopic measurements. Because the isotopic abundances of both ^{168}Yb and ^{170}Yb are originally small, 0.13% and 3.04% of the total, respectively, careful and precise measurements should be required to detect their variations. The expected variations for ^{168}Yb and ^{170}Yb isotopic abundances can be considered as follows:

$$\left(\frac{^{168}\mathrm{Yb}}{^{174}\mathrm{Yb}}\right) = \left(\frac{^{168}\mathrm{Yb}}{^{174}\mathrm{Yb}}\right)_0 \cdot e^{-\sigma\Psi} \tag{6}$$

$$\left(\frac{^{170}\mathrm{Yb}}{^{174}\mathrm{Yb}}\right) = \left(\frac{^{170}\mathrm{Yb}}{^{174}\mathrm{Yb}}\right)_0 + \left(\frac{^{169}\mathrm{Tm}}{^{174}\mathrm{Yb}}\right)_0 \cdot \left(1 - e^{-\sigma\Psi}\right) \tag{7}$$

where subscript 0 means a nonirradiated situation, Ψ is a total neutron fluence including thermal and epithermal fluence ($\Psi=\Psi_{th}+\Psi_{epi}$); σ is the total neutron-capture cross section including thermal and epithermal neutron-capture cross section ($\sigma=\sigma_{th}+\sigma_{epi}$). Here, $\sigma\Psi$ can be simply treated as $\sigma\Psi=\sigma_{th}\Psi_{th}+\sigma_{epi}\Psi_{epi}$. In this study, using two examples for the detectable Yb isotopic variations caused by neutron-capture reactions, one from the A-15 lunar regolith samples (Hidaka et al. 2020) and the other from the Oklo natural fission reactor samples (Holliger and Devillers 1981; Hidaka and Holliger 1998), the relationship between Ψ, σ, and isotopic variations of ^{168}Yb and ^{170}Yb is discussed by comparing the measured and calculated isotopic data.

Chemical separation of individual REEs for isotopic analyses

For the precise determination of Yb isotopic composition by mass spectrometric techniques, it is required to purify the Yb component after the separation of Er and Lu in the individual samples to completely avoid the isobaric interferences of all Yb isotopes on the mass spectra. Mizutani et al. (2020) established a chemical separation method for La, Ce, Nd, Sm, Gd, Dy, Er, Yb, and Lu without any isobaric interferences from other elements using column chromatography with lanthanide-specific (LN) resin (particle size of 20–50 μm) and HCl as the eluent. This method has been used conveniently for the chemical separation of Sm, Gd, Er, and Yb in a sequential procedure. In this technique, the elution behaviors of Pr, Eu, Tb, Ho, and Tm were not examined, because such five elements do not provide any isobaric interferences with the other elements on the mass spectra. Even if there are no isobaric interferences, the presence of impurities in a target element fraction significantly reduces the ionization efficiency during the isotopic analysis by a thermal ionization mass spectrometer. Therefore, it is desirable to separate any impurity elements from the target element as much as possible for better isotopic analyses. In this study, a part of the chemical separation technique for individual REEs given by Mizutani et al. (2020) was improved for better purification of Sm, Gd, Er and Yb fractions by the fine adjustments of the concentrations and flow volumes of HCl for Ln-resin packed column.

Isotopic analyses of Yb

Before starting this study, the isotopic measurement of Yb was given by the normal mode of a TRITON Plus thermal ionization mass spectrometer (TIMS) equipped with nine Faraday cups connected to individual 10^{11} Ω resistor amplifiers (Mizutani et al. 2020; Hidaka et al. 2020). This study used two of nine amplifiers modified to 10^{13} Ω

resistor amplifiers for the detection of ^{168}Yb and ^{170}Yb isotopes and the rest seven 10^{11} Ω resistor amplifiers for the detection of other five $^{171, 172, 173, 174, 176}$Yb isotopes and for the monitoring of ^{167}Er and ^{175}Lu to correct isobaric interferences to perform high-accuracy and precise Yb isotopic analyses.

Results and discussions

Yb isotopic data of the A-15 lunar regolith materials

The isotopic variations of ^{168}Yb/^{174}Yb and ^{170}Yb/^{174}Yb for individual samples are expressed as the deviation relative to those for the Yb standard reference material in ε-unit. The ε expression is defined as follows:

$$\varepsilon_{^{i}\mathrm{Yb}} = \left\{ \frac{\left(^{i}\mathrm{Yb}/^{174}\mathrm{Yb}\right)_{meas} - \left(^{i}\mathrm{Yb}/^{174}\mathrm{Yb}\right)_{\mathrm{std}}}{\left(^{i}\mathrm{Yb}/^{174}\mathrm{Yb}\right)_{\mathrm{std}}} \right\} \times 10^{4} \quad (8)$$

where $i = 168$ or 170, the subscripts "std" and "meas" mean standard reference materials without neutron irradiation and each sample used in this study, respectively.

The calculated ε values from the expected $\Psi_{th} + \Psi_{epi}$ and the measured ε values for seven samples from the A-15 lunar regolith samples are listed in Table 2. Considering the contribution of only Ψ_{th} estimated from the Sm isotopic shifts (Hidaka et al. 2000), the ε_{168Yb} values range from −1.2 to −1.7, which are much fewer variations compared with those of the A-15 samples by measurements (−12.7 to −27.9). The ε_{168Yb} values for the A-15 samples can be well reproduced by the contribution of Ψ_{epi} in addition to Ψ_{th}. Although the measured ε_{168Yb} data include large analytical uncertainties (±9 to 21 in ε unit), the estimated ε_{168Yb} ranges from −20 to −31 which is almost consistent with the measured ε_{168Yb} values within the analytical uncertainties.

The measured ε_{170Yb} excesses over the analytical uncertainties were not clearly detected in all of the A-15 samples (Hidaka et al. 2020). Considering the contribution of Ψ_{th} only, the ε_{170Yb} values estimated from Eq. (7) are less than +0.42 for all seven samples. These excesses cannot be detected by the current techniques, because the analytical uncertainties (±0.47 to 0.77 in ε unit) are over

Table 2 Comparison of the isotopic variations of (a) ^{168}Yb/^{174}Yb and (b) ^{170}Yb/^{174}Yb between measured and calculated values for seven of lunar regolith materials from the A-15 drill stem

Sample	Measured[a]		Calculated[b]		Calculated[c]		
	^{168}Yb/^{174}Yb	ε_{168Yb}	Ψ_{th}	ε_{168Yb}	Ψ_{th}	Ψ_{epi}	ε_{168Yb}
(a) ^{168}Yb/^{174}Yb							
STD	0.003956 ± 2	0	0	0	0	0	0
15001	0.003951 ± 8	−13 ± 21	5.2	−1.2	4.8	59	−22
15002	0.003951 ± 7	−13 ± 18	5.9	−1.4	5.7	67	−25
15003	0.003946 ± 5	−25 ± 14	6.9	−1.6	6.3	71	−27
15004	0.003945 ± 3	−28 ± 9	7.5	−1.7	6.9	81	−31
15005.14	0.003945 ± 5	−28 ± 14	7.0	−1.6	6.5	77	−29
15005.79	0.003947 ± 5	−23 ± 14	6.6	−1.5	6.1	75	−28
15006	0.003951 ± 5	−13 ± 14	5.5	−1.3	5.1	54	−20
Sample	**Measured[a]**		**Calculated[b]**		**Calculated[c]**		
	^{170}Yb/^{174}Yb	ε_{170Yb}	Ψ_{th}	ε_{170Yb}	Ψ_{th}	Ψ_{epi}	ε_{170Yb}
(b) ^{170}Yb/^{174}Yb							
STD	0.094812 ± 2	0	0	0	0	0	0
15001	0.094814 ± 6	+0.21 ± 0.67	5.2	+0.29	4.8	59	+6.4
15002	0.094814 ± 6	+0.21 ± 0.67	5.9	+0.33	5.7	67	+7.3
15003	0.094815 ± 7	+0.32 ± 0.77	6.9	+0.39	6.3	71	+7.8
15004	0.094810 ± 4	−0.21 ± 0.47	7.5	+0.42	6.9	81	+8.9
15005.14	0.094813 ± 5	+0.11 ± 0.57	7.0	+0.39	6.5	77	+8.4
15005.79	0.094809 ± 7	−0.32 ± 0.77	6.6	+0.37	6.1	75	+8.2
15006	0.094811 ± 4	−0.11 ± 0.47	5.5	+0.31	5.1	54	+5.9

STD means standard reference materials of Yb

[a] The data fromHidaka et al. (2020)

[b] The calculations were done under consideration of the contribution of Ψ_{th} only. The Ψ_{th} values (in 10^{16} *n* cm^{-2} unit) were given by Hidaka et al. (2000)

[c] The calculations were done under consideration of the contributions of both Ψ_{th} and Ψ_{epi}. Both Ψ_{th} and Ψ_{epi} values (in 10^{16} *n* cm^{-2} unit) were given by Hidaka et al. (2020)

the range of the estimated ε_{170Yb}. Considering the contributions of both Ψ_{epi} and Ψ_{th} (see Table 2), however, the estimated ε_{170Yb} ranging from + 5.9 to + 8.9 should be detectable enough even with the current analytical uncertainties.

The results from the comparison between the measured and calculated Yb isotopic variations reveal that ^{168}Yb is affected by both Ψ_{th} and Ψ_{epi}, and that ^{170}Yb is affected by only Ψ_{th}. How should this inconsistency be interpreted? One of the ideas to explain this issue is the estimation of σ_{epi} by Eq. (2). In this study, σ_{epi} is simply calculated from Eq. (2) based on individual RI and E_{max} values. The measured isotopic data of ^{170}Yb/^{174}Yb suggest that epithermal neutrons did not interact sufficiently with ^{169}Tm. The resonance region of the neutron-capture cross section for ^{169}Tm is wider (0.1 < RI < 2000 eV) than that of ^{168}Yb (0.5 < RI < 200 eV); therefore, if the energy distribution of epithermal neutrons at the lunar surface is deviated to the lower energy region rather than 2000 eV, the effective σ_{epi} for ^{169}Tm should be less than our estimation. If the energy of most neutrons arising on the lunar surface does not reach 2000 eV, the effective cross section of ^{169}Tm should be estimated to be less than 1.95×10^2 barn.

In the current situation, it is experimentally unclear whether the ^{170}Yb isotope reacts sufficiently with epithermal neutrons. Through the isotopic study of the A-15 regolith core, Ψ is estimated to be of the 10^{16} order (Russ et al. 1972; Hidaka et al. 2000). In the second example, it is interesting to consider the relationship between Ψ, σ_{th}, and σ_{epi} for the Oklo natural reactor materials. The total neutron fluences of the Oklo reactors, including thermal and epithermal neutrons, are estimated to be in the range of 10^{20} to 10^{21} n cm^{-2} (Holliger and Devillers 1981; Gauthier-Lafaye et al. 1996; Hidaka and Holliger 1998). The isotopic variations of ^{168}Yb and ^{170}Yb can be clearly shown in the Oklo natural reactor materials. In the case of the Oklo reactor samples, their isotopic variations are so large that it is convenient to discuss using isotopic ratios instead of ε-notation.

Yb isotopic data of the Oklo natural fission reactor

The Oklo uranium deposit in the Republic of Gabon, Central Africa, is known as a fossil of natural fission reactor. The isotopic compositions of many elements have varied with the occurrence of several types of nuclear reactions in the reactor zones. Two major reactions occurred in the Oklo reactors: a fission reaction mainly of ^{235}U induced by thermal neutrons and the neutron-capture reactions of many nuclides existing in the reactor with neutrons released by the fission reactions. The neutron fluences arising in the Oklo reactors are quantitatively estimated to be 10^{20}–10^{21} n cm^{-2} (Gauthier-Lafaye et al. 1996; Hidaka and Holliger 1998). Since the nuclides with mass numbers 130 to 150 corresponding to lighter to middle REEs such as La, Ce, Pr and Nd have high fission product yields by fission reactions, significant amounts of fissiogenic components were produced and mixed with originally existing components that had been included since the ore formation. As a result, isotopic compositions of lighter to middle REEs vary not only with the contribution of neutron-capture reactions but also with the contribution of fission reactions. On the other hand, isotopic compositions of heavier REEs like Er, Yb, and Lu in the Oklo reactor materials were affected mainly by neutron-capture reactions because of the extremely low fission product yields of the nuclides with mass numbers over 150 belonging to Er, Yb and Lu. The isotopic composition of Yb from the Oklo reactor materials is the best example of the isotopic shifts associated with neutron-capture reactions under intensive neutron irradiations.

In previous studies, Yb isotopic analyses were performed on nine samples collected from several locations of the natural fission reactors (Holliger and Devillers 1981; Hidaka and Holliger 1998). The results of ^{168}Yb/^{174}Yb and ^{170}Yb/^{174}Yb isotopic ratios for the nine samples are listed in Table 3. All nine samples have clear variations of the depletion of ^{168}Yb and the excess of ^{170}Yb for individual samples, although ^{168}Yb/^{174}Yb isotopic ratios for six of nine samples show the detection limits below 0.001 because of the intense depletions of ^{168}Yb isotope. The Ψ values of individual reactor samples were already obtained from previous studies; hence, the ^{168}Yb/^{174}Yb and ^{170}Yb/^{174}Yb isotopic ratios could be simulated by substituting the estimated Ψ values into Eqs. (6) and (7). The Ψ values used for the calculation are also listed in the table. As a result of the calculation, any Ψ values used for the calculation were insufficient to satisfy the isotopic variations of both ^{168}Yb and ^{170}Yb. The difference between the measured and calculated isotopic variations of both ^{168}Yb and ^{170}Yb for each sample is considered to be corrected by the addition of the Ψ_{epi} value. The additional Ψ_{epi} values to satisfy the variations of ^{168}Yb and ^{170}Yb for individual samples are calculated based on Eqs. (6) and (7). The results are listed in Table 3.

In the Oklo studies, the neutron-capture reaction of ^{143}Nd has been conventionally used to estimate the neutron fluence arising in the reactor (Ruffenach et al. 1976). In this estimation of the neutron fluence, the proportion of epithermal neutrons to thermal neutrons has been quantified as a neutron spectrum index. Previous studies suggested that the neutrons generated in the Oklo reactors were well-thermalized and that the thermalized neutrons worked sufficiently to sustain the criticality for fission. As shown in Table 3, the proportion of Ψ_{epi} to Ψ by conventional method was at least 10%.

Table 3 The results of calculated $^{168}Yb/^{174}Yb$ and $^{170}Yb/^{174}Yb$ isotopic ratios from the estimated neutron fluences (Ψ:10^{20} *n* cm^{-2}) and calculated neutron fluences from the measured Yb isotopic ratios for nine of the Oklo natural reactor materials

Sample	Referred[a]		Calculated[b]		Measured[a]		Calculated[c]	
	Ψ_{th}	Ψ_{epi}	$^{168}Yb/^{174}Yb$	$^{170}Yb/^{174}Yb$	$^{168}Yb/^{174}Yb$	$^{170}Yb/^{174}Yb$	Ψ_{th}	Ψ_{epi}
STD	0	0	0.003956	0.094801	0.003956	0.094801	0	0
SC55-1852	1.18	0.066	0.002944	0.102858	0.002056	0.111322	2.47	0.21
KN267-2194	4.02	0.347	0.001386	0.123073	< 0.001	0.180793	NA	NA
KN245-2674	1.91	0.100	0.002461	0.107669	0.001489	0.120051	2.99	0.73
KN250-2682	1.05	0.045	0.003056	0.101829	0.002731	0.105047	1.28	0.21
SF84-1469	4.87	0.380	0.001128	0.128416	< 0.001	0.183674	NA	NA
SF84-1480	7.62	0.364	0.000603	0.144095	< 0.001	0.204620	NA	NA
SF84-1485	5.87	0.354	0.000905	0.133937	< 0.001	0.177657	NA	NA
SF84-1492	5.29	0.353	0.001035	0.130561	< 0.001	0.183774	NA	NA
SD37	7.06	0.736	0.000600	0.144886	< 0.001	0.245122	NA	NA

STD means a standard reference materials of Yb

Ψ_{th} and Ψ_{epi} are expressed in 10^{20} (n cm^{-2}) unit

[a] The data for the estimated Ψ_{th} and Ψ_{epi}, and measured isotopic ratios of $^{168}Yb/^{174}Yb$ and $^{170}Yb/^{174}Yb$ are given by Holliger and Devillers (1981) and Hidaka and Holliger (1998)

[b] The isotopic ratios were calculated by substituting the estimated Ψ_{th} and Ψ_{epi} into Eqs. (6) and (7)

[c] The neutron fluences were calculated by substituting the measured $^{168}Yb/^{174}Yb$ and $^{170}Yb/^{174}Yb$ isotopic ratios into Eqs. (6) and (7)

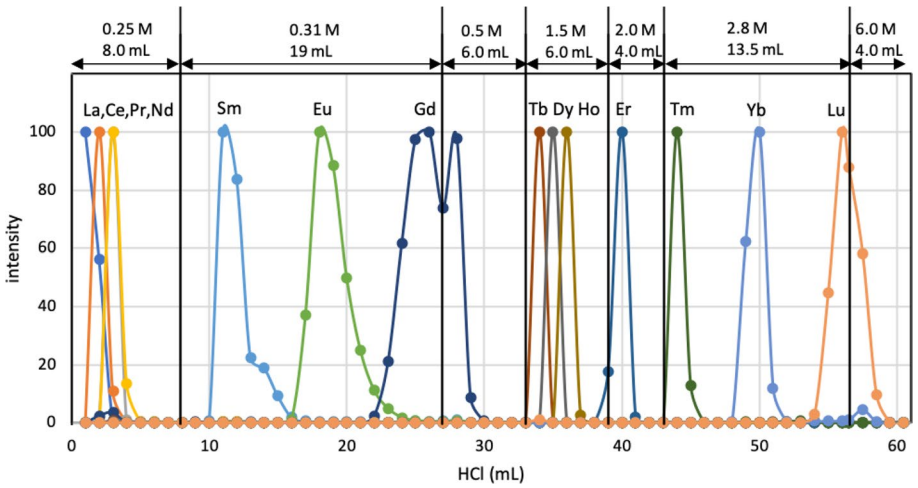

Fig. 2 Elution behaviors of individual REEs by 7-step of sequential separation using an Ln-resin packed column with HCl. The method partialy modified previous study by Mizutani et al. (2020)

However, according to our calculation in this study, the isotopic variations of both ^{168}Yb and ^{170}Yb cannot be produced only from the Ψ estimated by previous studies, but require additional neutron-capture reactions supported by an additional amount of Ψ_{epi}.

In this study, the evaluations of Ψ_{th} and Ψ_{epi} for the Oklo reactor materials only from the Yb isotopic data were examined as a new attempt. The data for the $^{168}Yb/^{174}Yb$ and $^{170}Yb/^{174}Yb$ isotopic ratios listed in Table 3 were substituted into Eqs. (6) and (7). As a result, the neutron fluences of $\Psi_{th} = (1.3–3.0) \times 10^{20}$ and $\Psi_{epi} = (2.1–7.3) \times 10^{18}$ n cm^{-2} are evaluated for three of nine samples, SC55, KN245, and KN250. On the other hand, the neutron fluences of the other six samples cannot be fixed because of a lack of the proper $^{168}Yb/^{174}Yb$ ratios. These isotopic data were given by classic mass spectrometric techniques more than 25 years ago. Assuming the $^{168}Yb/^{174}Yb$ isotopic ratios of the Oklo reactor materials can be determined precisely, the isotopic variations of the pair of ^{168}Yb and ^{170}Yb may be

Table 4 The procedures of column chemistry for the separation of Sm, Gd, Er and Yb

Procedure	Eluent	Volume (mL)	Remarks
Cleaning	6.0 M HCl	2.5	
Conditioning	Milli-Q water	2.5	
	0.25 M HCl	2.5	
Load sample		1 drop	
Waste	0.25 M HCl	8.0	Elution of La, Ce, Pr and Nd
Waste	0.31 M HCl	1.0	
Collect Sm	0.31 M HCl	8.0	
Waste	0.31 M HCl	4.0	Elution of Eu
Collect Gd	0.31 M HCl	6.0	
Collect Gd	0.5 M HCl	4.0	
Waste	0.5 M HCl	2.0	
Waste	1.5 M HCl	4.0	Elution of Tb, Dy and Ho
Collect Er	1.5 M HCl	2.0	
Collect Er	2.0 M HCl	3.0	
Waste	2.0 M HCl	1.0	
Waste	2.8 M HCl	3.5	Elution of Tm
Collect Yb	2.8 M HCl	6.0	

used as the dosimetry for Ψ_{th} and Ψ_{epi}. The Yb isotopic variation of the sample SD37 and its relationship with the neutron fluences is of particular interest, because SD37 locating at the reactor zone 13 at Oklo is considered to have experienced the highest neutron including fast neutrons studied from some isotopic studies (Meshik et al. 2004; Groopman et al. 2018; Hidaka et al. 2023).

Development of precise isotopic measurements of Yb

For the chemical separation of Sm, Gd, Er and Yb, an Ln-resin packed column (particle size of 20–50 mm, column volume of 0.5 mL, column size of 110 mm-length and 2.5 mm-diameter) was used in this study. Figure 2 shows the elution behaviors of individual REEs from Sm to Lu after several adjustments to achieve better conditions. The purifications of Sm, Gd, Er, and Yb are much improved by the complete separation of isobaric interferences as well as the other elements as much as possible. The recovery yields of Sm, Gd, Er, and Yb are more than 98%. The detailed procedures for the collection of Sm, Gd, Er and Yb are given in Table 4.

Table 5 shows a preliminary result of comparison for the Yb isotopic data set collected by the use of all nine 10^{11} Ω resistor amplifiers and the use of two 10^{13} Ω resistor amplifiers plus seven 10^{11} Ω resistor amplifiers. In addition to the results of 5 repeated analytical runs of Yb standard material (1000 mg/L of single-element standard solution for the ICP-MS and ICP-AES analyses provided by SPEX CertiPrep), their analytical uncertainties of the average values are shown in 2SD (standard deviation) in the table. As a result of a simple comparison between two data sets, the analytical precisions for $^{168}Yb/^{174}Yb$ and $^{170}Yb/^{174}Yb$ isotopic ratios using 10^{13} Ω resistor amplifiers show about five and two times better, respectively, than those by the conventional method. Assuming these analytical precisions can be practically reproduced for planetary materials, the neutron fluence of $\Psi > 2 \times 10^{16}$ n cm^{-2} can be detectable. While the

Table 5 Comparison of the data sets for Yb isotopic ratios collected from two different methods

	$^{168}Yb/^{174}Yb$	$^{170}Yb/^{174}Yb$	$^{171}Yb/^{174}Yb$	$^{173}Yb/^{174}Yb$	$^{176}Yb/^{174}Yb$
Method1*					
run1	0.0039578 ± 0.0000007	0.0948014 ± 0.0000012	0.4459279 ± 0.0000029	0.5050452 ± 0.0000021	0.4022459 ± 0.0000029
run2	0.0039534 ± 0.0000009	0.0948033 ± 0.0000013	0.4459327 ± 0.0000024	0.5050415 ± 0.0000019	0.4022469 ± 0.0000024
run3	0.0039548 ± 0.0000012	0.0948025 ± 0.0000017	0.4459324 ± 0.0000034	0.5050455 ± 0.0000026	0.4022436 ± 0.0000035
run4	0.0039587 ± 0.0000012	0.0948099 ± 0.0000021	0.4459335 ± 0.0000045	0.5050457 ± 0.0000034	0.4022437 ± 0.0000043
run5	0.0039646 ± 0.0000007	0.0948046 ± 0.0000011	0.4459318 ± 0.0000022	0.5050471 ± 0.0000017	0.4022466 ± 0.0000023
Average	0.0039579 ± 0.0000087	0.0948043 ± 0.0000066	0.4459317 ± 0.0000044	0.5050450 ± 0.0000042	0.4022453 ± 0.0000032
Method2**					
run1	0.0039577 ± 0.0000002	0.0948024 ± 0.0000006	0.4459353 ± 0.0000036	0.5050465 ± 0.0000026	0.4022467 ± 0.0000037
run2	0.0039563 ± 0.0000003	0.0948034 ± 0.0000007	0.4459343 ± 0.0000032	0.5050478 ± 0.0000023	0.4022474 ± 0.0000032
run3	0.0039579 ± 0.0000005	0.0947982 ± 0.0000010	0.4459282 ± 0.0000028	0.5050480 ± 0.0000022	0.4022467 ± 0.0000031
run4	0.0039553 ± 0.0000002	0.0948001 ± 0.0000008	0.4459283 ± 0.0000029	0.5050373 ± 0.0000022	0.4022494 ± 0.0000032
run5	0.0039556 ± 0.0000003	0.0948013 ± 0.0000006	0.4459339 ± 0.0000023	0.5050449 ± 0.0000023	0.4022420 ± 0.0000025
Average	0.0039566 ± 0.0000024	0.0948011 ± 0.0000041	0.4459320 ± 0.0000069	0.5050449 ± 0.0000089	0.4022464 ± 0.0000054

The numbers of uncertainties for individual analytical runs are shown as 2SE

The numbers of uncertainties for the average values are shown as 2SD

*Use of 10^{11} Ω resistor amplifiers for detection of all Yb isotopes

**Use of two 10^{13} Ω resistor amplifiers for detection of ^{168}Yb and ^{170}Yb isotopes and use of seven 10^{11} Ω resistor amplifiers for detection of other five Yb isotopes and two background

use of 10^{13} Ω resistor amplifiers has the advantage to enhance the abundance sensitivity for the detection of small ion beam like $^{168, 170}$Yb isotopes, it has disadvantage to reduce the precision of gain factors of 10^{11} Ω resistor amplifiers for the detection of other five ^{171,172,173,174,176}Yb isotopes because of the replacement of conventional gain calibration board supplying a current of 330 pA into a new one supplying 3.3 pA. In addition, significant time variations of the electronic baseline noise and relative gain factors during a few months after the installation are also reported (Torrano et al. 2023). Further studies are required to achieve higher precision of ^{168}Yb/^{174}Yb and ^{170}Yb/^{174}Yb isotopic ratios.

Summary

Several nuclear reactions that occurred in nature have been applied for the characterization of planetary materials. In this paper, isotopic variations caused by neutron-capture reactions were examined from the viewpoint of the interaction of cosmic-ray with planetary surfaces in space. The combination of isotopic shifts of ^{149}Sm–^{150}Sm, ^{157}Gd–^{158}Gd and/or ^{167}Er–^{168}Er in association with neutron-capture reactions has been used to estimate the neutron fluence and energy balance between thermal and epithermal neutrons. The results can be effectively used to understand the CRE history and situations for individual planetary materials. Although it is still in the process of developing precise isotopic measurement of Yb, the possibility and potential of effective use of Yb isotopic variations in association with neutron-capture reactions are quantitatively discussed from the numerical simulation using isotopic data from the A-15 lunar regolith and the Oklo natural reactor materials.

Author contributions

HH designed the research, conducted the experiments and wrote the manuscript.

Funding

This work was supported by Grant-in-Aid for the Japan Society for the Promotion of Science (JSPS) Scientific Research (A) Grant No. JP22H00174 awarded to Hiroshi Hidaka.

Availability of data and materials

All data generated or analyzed during this study are included in this published article [and its supplementary information files].

Declarations

Competing interests

The authors declare that they have no competing interests.

Received: 7 November 2023 Accepted: 6 March 2024
Published online: 19 March 2024

References

Albalat E, Telouk P, Albarède F. Er and Yb isotope fractionation in planetary materials. Earth Planet Sci Lett. 2012. https://doi.org/10.1016/j.epsl.2012.08.021.

Albalat E, Blichert-Toft J, Telouk P, Albarède F. The lunar neutron energy spectrum inferred from the isotope compositions of rare-earth elements and hafnium in Apollo samples. Earth Planet Sci Lett. 2015. https://doi.org/10.1016/j.epsl.2015.07.056.

Amelin Y, Davis WJ. Geochemical test for branching decay of ^{176}Lu. Geochim Cosmochim Acta. 2005. https://doi.org/10.1016/j.gca.2004.04.028.l.

Gauthier-Lafaye F, Holliger P, Blanc PL. Natural fission reactors in the Franceville basin. Geochim Cosmochim Acta. 1996. https://doi.org/10.1016/S0016-7037(96)00245-1.

Groopman EV, Willingham DG, Meshik AP, Pravdivtseva OV. Discovery of fissiogenic Cs and Ba capture five years after Oklo reactor shutdown. PNAS. 2018. https://doi.org/10.1073/pnas.1807267115.

Hidaka H, Holliger P. Geochemical and neutronic characteristics of the natural fossil fission reactors at Oklo and Bangombé. Gabon Geochim Cosmochim Acta. 1998. https://doi.org/10.1016/50016-7037(97)00319-0.

Hidaka H, Ebihara M, Yoneda S. Neutron capture effects on samarium, europium, and gadolinium in Apollo 15 deep drill-core samples. Meteor Planet Sci. 2000. https://doi.org/10.1111/j.1945-5100.2000.tb01438.x.

Hidaka H, Mizutani Y, Yoneda S. Estimation of thermal and epithermal neutron fluences at the lunar surface from isotopic compositions of rare earth elements. Astrophys J. 2020. https://doi.org/10.3847/1538-4357/abbffe.

Hidaka H, Bentridi SE, Gall B. Evidence of fast neutron operating in Oklo. Radiat Prot Dosimetry. 2023. https://doi.org/10.1093/rpd/ncad015.

Holliger P, Devillers C. Contribution à l'étude de la température dans les réacteurs fossils d'Oklo par la mesure du rapport isotopique du lutétium. Earth Planet Sci Lett. 1981. https://doi.org/10.1016/0012-821X(81)90209-0.

Lingenfelter RE, Canfield EH, Hampel VE. The lunar neutron flux revisited. Earth Planet Sci Lett. 1972. https://doi.org/10.1016/0012-821X(72)90153-7.

Meshik AP, Hohenberg CM, Pravdivtseva OV. Record of cycling operation of the natural nuclear reactor in the Oklo/Okelobondo area in Gabon. Phys Rev Lett. 2004. https://doi.org/10.1103/PhysRevLett.93.182302.

Mizutani Y, Hidaka H, Yoneda S. Chemical separation and determination of the isotopic compositions of dysprosium, erbium and ytterbium in geological materials by thermal ionization mass spectrometry. Geochem J. 2020. https://doi.org/10.2343/geochemj.2.0609.

Nishiizumi K, Caffee MW, Jull ATJ, Reedy RC. Exposure history of lunar meteorites Queen Alexandra Range 93069 and 94269. Meteor Planet Sci. 1996. https://doi.org/10.1111/j.1945-5100.1996.tb02122.x.

Ruffenach JC, Menes J, Devillers C, Lucas M, Hagemann R. Etudes chimiques et isotopiques de l'uranium, du plomb et de plusieurs produits de fission dans un echantillon de minerai du reacteur naturel d'Oklo. Earth Planet Sci Lett. 1976. https://doi.org/10.1016/0012-821X(72)90011-X.

Russ GP, Burnett DS, Wasserburg G. Lunar neutron stratigraphy. Earth Planet Sci Lett. 1972. https://doi.org/10.1016/0012-821X(72)90058-1.

Shollenberger Q, Brennecka GA. Dy, Er, and Yb isotopic compositions of meteorites and their components: Constraints on presolar carriers of the rare earth elements. Earth Planet Sci Lett. 2020. https://doi.org/10.1016/j.epsl.2019.115866.

Shollenberger Q, Render J, Brennecka GA. Er, Yb, and Hf isotopic compositions of refractory inclusions: an integrated isotopic fingerprint of the solar system's earliest reservoir. Earth Planet Sci Lett. 2018. https://doi.org/10.1016/j.epsl.2018.05.007.

Spergel MS, Reedy RC, Lazareth OW, Levy PW, Slatest LA. Cosmogenic neutron-capture-produced nuclides in stony meteorites. J Geophys Res. 1986. https://doi.org/10.1029/JB091iB04p0D483.

Torrano ZA, et al. Neodymiumu-142 and samarium neutron stratigraphy of C-type asteroid (162173) Ryugu. Meteor Planet Sci. 2023. https://doi.org/10.1111/maps.14109.

Publisher's Note